RSC Advances

PAPER

Cite this: *RSC Adv.*, 2023, **13**, 4890

Catalytic behavior of a ZnO/TiO_2 composite in the synthesis of polycarbonate diol†

Ran Chong,[a] Fei Qian,[b] Zhong-Hua Sun,*[a] Mei-Jun Wei,[a] Wei-You Zhou,[a] Jing Zhang,[a] Ming-Yang He,[a] Qun Chen[a] and Jun-Feng Qian*[a]

Received 26th November 2022
Accepted 22nd December 2022

DOI: 10.1039/d2ra07527j

rsc.li/rsc-advances

ZnO/TiO_2 catalysts with different ZnO contents have been prepared through equal volume impregnation method, characterized by XRD, SEM, Py-IR, ICP, XPS, NH_3-TPD and N_2 adsorption/desorption, and evaluated in the synthesis of polycarbonate diol (PCDL) through transesterification. The results showed that titanium zinc oxide formed in these catalysts, and the content of acidic sites varied with the ZnO content, and ZnO/TiO_2 (10%) has the highest acid amount. The ZnO/TiO_2 (20%) with medium acidic sites showed the highest catalytic activity. The synthesis process of polycarbonate glycol was also optimized. Under the optimal reaction conditions, the yield of PCDL was 72.5%, and the M_n reached 4829 g mol^{-1} with a PDI of 1.6.

1. Introduction

Polycarbonate diol (PCDL) is an oligomer polyol with a regular molecular structure and a repeating carbonate group in the main chain.[1] The carbonate group has the characteristics of large polarity and high cohesion energy, and it is easy to form intermolecular hydrogen bonds, so that PCDL has good mechanical properties, wear resistance and oil resistance. The small steric resistance of carbonate bonds also allows some molecular chain segments to rotate and vibrate, thus giving PCDL low temperature compliance.[2] In recent years, the polycarbonate glycol (PCDL) market consumption has grown rapidly; the main downstream uses are in electronic appliances, plates and automobiles, the other main use is for blending with other polymers, such as the production of polyethylene terephthalate and polyether.[3–6] In summary, PCDL has received widespread attention in the industry for its excellent performance.

The synthesis of PCDL by phosgene method is seriously polluting the environment, so it has been gradually eliminated.[7,8] The non-phosgene method mainly includes cyclic carbonate open-ring copolymerization method, carbon dioxide epoxy copolymerization method and transesterification method.[9] The cyclic carbonate open-loop copolymerization method has the problem of equilibrium between the cyclic reaction and the polymerization reaction.[10,11] And the carbon dioxide epoxy copolymerization method can only synthesize PCDL with specific epoxide structure. Transesterification method normally catalysts use to be added in little amount only, mild reaction conditions, flexibility for preparing PCDLs with multiple structures, and controllability of relative molecular mass of the target products.[12,13] Therefore, transesterification is considered to be a promising method of PCDL synthesis.

CH_3COONa,[13] tetrabutyl titanate(IV),[14] $Zn(OAc)_2$ (ref. 15) and $(CH_3COO)_2Mg$[16] are commonly used as homogeneous catalysts in transesterification and exhibit excellent catalytic activity, but it is difficult to separate and regenerate from the products. In this context, the development of heterogeneous catalysts is desirable considering the demerits of homogeneous catalysts.[17] Several heterogeneous catalysts have been reported in literature. For example, Wang *et al.*[9] synthesized Mg–Fe/Ti layered double hydroxides (LDHs) for the transesterification between dimethyl carbonate (DMC) and aliphatic diols. Under optimal conditions with a catalyst amount of 1 wt%, the number-average molecular weight (M_n) of PCDL reached 3030 g mol^{-1}, the yield of PCDL was 89.1%. Unfortunately, due to the formation of azeotrope between methanol and DMC during the reaction, it is difficult to control the M_n of the target product.[18] In order to address these problems, the synthesis of PCDL using diphenyl carbonate (DPC) are disclosed.[19] Therefore, the development of effective heterogeneous catalysts is of great significance for the synthesis of PCDL by transesterification of DPC with BDO.

TiO_2 is commonly used as a heterogeneous support due to its high surface area and good availability.[20–22] TiO_2 loaded with metallic oxide, such as La,[23] Pt,[24] Pt–Ru Bi metal alloy,[25] Fe and Cu,[26] and Zn[27–33] have been widely used in photocatalysis field. Chen *et al.*[34] synthesized a catalyst of SO_4^{2-} loaded on TiO_2 for transesterification in the production of biodiesel. On the other hand, various catalysts has also been prepared based on ZnO for

[a]Jiangsu Key Laboratory of Advanced Catalytic Materials and Technology, Advanced Catalysis and Green Manufacturing Collaborative Innovation Center, Changzhou University, Changzhou 213164, China. E-mail: sunzhonghua@cczu.edu.cn; qianjunfeng@cczu.edu.cn

[b]Jiangsu Lingfei Chemical Co., Ltd, Wuxi 214264, China

† Electronic supplementary information (ESI) available: GC-FID, XRD, FTIR and ^{1}H NMR. See DOI: https://doi.org/10.1039/d2ra07527j

transesterification,[35,36] because the rich oxygen vacancies on the surface of ZnO can enhance the Lewis acidity of the catalyst and improve the catalytic activity.[37] However, it is not easy to recycle, because ZnO is difficult to be extracted from the product. In order to solve the drawback, we envisioned that loading ZnO on TiO_2 would result in a recycled catalyst with high catalytic activity for the transesterification reaction.[38] In this work, ZnO/TiO_2 catalysts with different zinc mass fractions were prepared by equal volume impregnation, and the catalytic performance in the synthesis of PCDL *via* transesterification was evaluated. Furtherly, the transesterification process was also optimized.

2. Experimental

2.1 Materials

The chemical materials involved were obtained as follows: 1,4-butanediol ($C_4H_{19}O_2$, CP), tetrabutyl titanate ($C_{16}H_{36}O_4Ti$, AR), diphenyl carbonate ($C_{13}H_{10}O_3$, CP) and dichloromethane (CH_2Cl_2, AR) were purchased from Shanghai Lingfeng Chemical Reagent Co., Ltd, ethanol (C_2H_6O, 95%) was purchased from Jiangsu Yongfeng Co., Ltd, zinc nitrate hexahydrate [$Zn(NO_3)_2 \cdot 6(H_2O)$ AR], was purchased from Sinopharm Chemical Reagent Co., Ltd.

2.2 Preparation of catalysts

TiO_2 was prepared by hydrolysis method.[38,39] Mix 0.5 M tetrabutyl titanate with 7 M ethanol; mix 2 M deionized water with 7 M ethanol. In which the mixture of ionic water and ethanol was dripped into the mixture of tetrabutyl titanate and ethanol, constant stirring for about 1 hour and the mixture was aged at ambient temperature for 3 h. The precipitate was filtered out, dried, grounded into powder, and then calcined in a muffle furnace at 450 °C for 4 h to give TiO_2.

The ZnO/TiO_2 catalysts were prepared by an incipient wetness impregnation method. Taking the synthesis of 10% supported catalyst as an example, 0.005 M zinc nitrate hexahydrate dissolved in 0.2 M deionized water, and the aqueous solution of zinc nitrate hexahydrate slowly added dropwise to 0.05 M TiO_2, and stirred at ambient temperature for 3 h. After being filtered, the residue was dried, grinded, and then roasted at 450 °C in muffle furnace for 4 h. The obtained catalyst was denoted as ZnO/TiO_2 (20%). ZnO/TiO_2 (10%), ZnO/TiO_2 (30%) and ZnO/TiO_2 (40%) were prepared *via* the similar method.

2.3 Catalyst characterizations

X-ray diffraction (XRD) of the materials were carried out on a D/max 2500 PC diffractometer (Rigaku Company, Japan). The test conditions were Cu Kα radiation ($\lambda = 0.15406$ nm), 40 kV, 150 mA, 2θ 5°–80° and step length 0.02°. N_2 adsorption isotherms were measured on an ASAP2460 sorption analyzer (Micromeritics, Norcross, Georgia, USA). NH_3-TPD tests were performed on a CHEMBET3000 chemical adsorption instrument (Quantachrome Company, USA). Scanning electron microscope (SEM) of the materials were carried out on SUPRA55 instrument (Zeiss Company, Japan). X-ray photoelectron spectroscopy (XPS) of the materials were carried out on K-Alpha instrument (Thermo Fisher Scientific Company, USA). Test conditions: the excitation source was Al-Kα (1486.8 eV), the background vacuum was 5.0×10^{-7} mBar, and the variable carbon C 1s = 284.80 eV was used as the standard for nuclear power correction. Electron-coupled plasma atomic emission spectrometry (ICP) of the materials were carried out on Vista-AX instrument (Varian Company, USA). FT-IR spectra after adsorption of pyridine (Py-IR) of the materials were carried out on Nicolet 9700 instrument (Thermo Fisher Scientific Company, USA).

2.4 Reaction procedure and catalyst performance evaluation

In a typical process, DPC (107.1 g, 0.5 mol), BDO (49.6 g, 0.55 mol) and ZnO/TiO_2 (0.32 g, 0.3 wt%) catalyst were successively charged into a three-necked round-bottom flask, which was stirred and heated to melt under nitrogen protection. The total reaction time of synthesis PCDL is 6 h. Prepolymerization 3 h, polycondensation 3 h, in the polycondensation 3 h vacuum pumping to −0.095 MPa stop the reaction. The resulting mixture was dissolved in dichloromethane (2 equivalent) and the catalyst was filtered off for the next run, and PCDL product was precipitated upon adding excessive ethanol in the mixture.

The distillate was determined using a gas chromatograph (Agilent HP-5) fitted with a flame ionization detector (GC-FID). The column temperature was 120 °C and injection temperature was 320 °C.

The M_n and polydispersity index (PDI) were determined by gel permeation chromatography (GPC) at 40 °C in tetrahydrofuran. GPC analysis was carried out using a Shimadzu apparatus equipped with a LC-20AD HPLC pump, a refractive index detector (RID-10A, 120 V) and a Waters Styragel guard column (20 μm, 4.6 × 30 mm) followed by two Waters Styragel columns (HR 4E, 5 μm, mixed bed, 7.8 × 300 mm, and HR 5E, 5 μm, mixed bed, 7.8 × 300 mm). Tetrahydrofuran was used as eluent with a flow rate of 0.6 mL min^{-1} and calibrated with polystyrene standards (M_n = 1770, 17 300, 135 000 and 305 000 Da).

The product was dried in vacuum oven at 40 °C for 12 h and weighed. The yield was calculated by formula (1).

$$\text{Yield } (\%) = \frac{m}{m_t} \quad (1)$$

Among them, m (g) is the actual mass of the PCDL product and m_t (g) is the theoretical mass of the PCDL product.

3. Results and discussion

3.1 Catalyst characterization

As can be seen from Fig. 1, the catalysts with different ZnO mass fractions have characteristic diffraction peaks of anatase TiO_2 at 2θ of 25.4°, 37.8°, 48.3°, 54.2° and 63.1°. It is shown that the structure of the carrier does not change after ZnO loading and roasting, and the characteristic diffraction peaks of ZnO appear at 2θ of 34.6°, 36.4° and 56.6°. From the XRD spectra, it can be seen that Zn_4TiO_6 formed in different loading catalysts. With the increase of the loading amount of ZnO, the peak for the composite oxide gradually becomes sharper.[33,40]

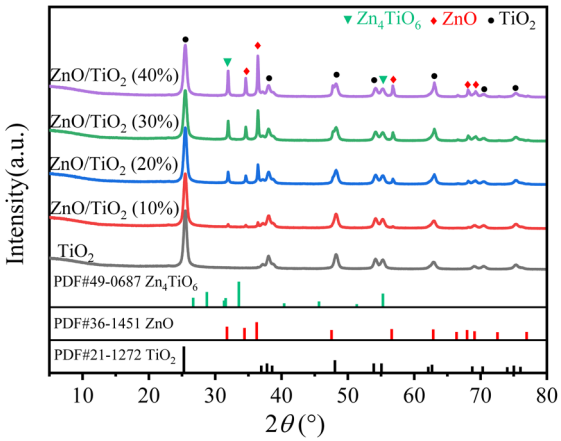

Fig. 1 XRD of ZnO/TiO_2 with different ZnO mass fractions.

The chemical environments of the titanium, oxygen and zinc were investigated by XPS (Fig. 2). Full-spectrum XPS (Fig. 2A) indicates the presence of Ti, Zn and O in the ZnO/TiO_2. The spectrum for Ti 2p (Fig. 2B) contains two peaks: the first one at about 463.98 eV refers to the Ti $2p_{1/2}$, and the second one at about 458.28 eV corresponds to the Ti $2p_{3/2}$.[41,42] XPS Zn 2p spectra (Fig. 2C) also show two peaks approximately at 1044.58 eV and 1021.48 eV, which are characteristics of Zn $2p_{1/2}$ and Zn $2p_{3/2}$, respectively,[27,32,41] and the energy interval between the peaks is ~23 eV. The above information confirms that Zn is completely oxidized and is in the +2-valence state.[39] The XPS spectra indicate the presence of Ti^{4+} for titanium, Zn^{2+} for zinc[28] on the surface of composites. It can be seen from Table 1 that the content of Zn on the catalyst surface increases slowly with the increase of ZnO loading. Among them, the surface Zn content increased the most when the ZnO loading increased from 10% to 20%. In addition, we investigated the O 1s XPS spectrum (Fig. 2D) of ZnO/TiO_2. Results show that the peak positioned at 529.48 eV is due to the lattice oxygen anions (O^{2-}) including Ti═O, Zn═O.[43] The peak at 531.28 eV corresponds to loosely bound oxygen species, such as C–O, C═O, H_2O, and OH groups.[44,45] The results illustrated that the samples were composited of metal oxides, namely that of Ti and Zn.

Comparison between the binding energy of TiO_2 and ZnO/TiO_2, the binding energy of TiO_2 increases significantly after loading ZnO, which demonstrates that positively charged Ti^{4+} and Zn^{2+} is enhanced. There is an interaction between titanium, zinc and oxygen on the catalyst, which leads to a deviation from the electron cloud of titanium and zinc.[46] Based on the above analysis, the heterostructures were formed in ZnO/TiO_2 composite due to that the well-defined morphology and intimate interfacial contact between TiO_2 and ZnO, in consistent with the XRD pattern. The ICP analysis show that the measured content of ZnO is slightly lower than the theoretical value (Table 1), indicating that not all the Zn was successfully loaded into TiO_2.

3.2 Analysis of surface acidity

NH_3-TPD analysis of ZnO/TiO_2 samples with different ZnO mass fractions and the Py-IR curve of ZnO/TiO_2 (20%) are depicted in

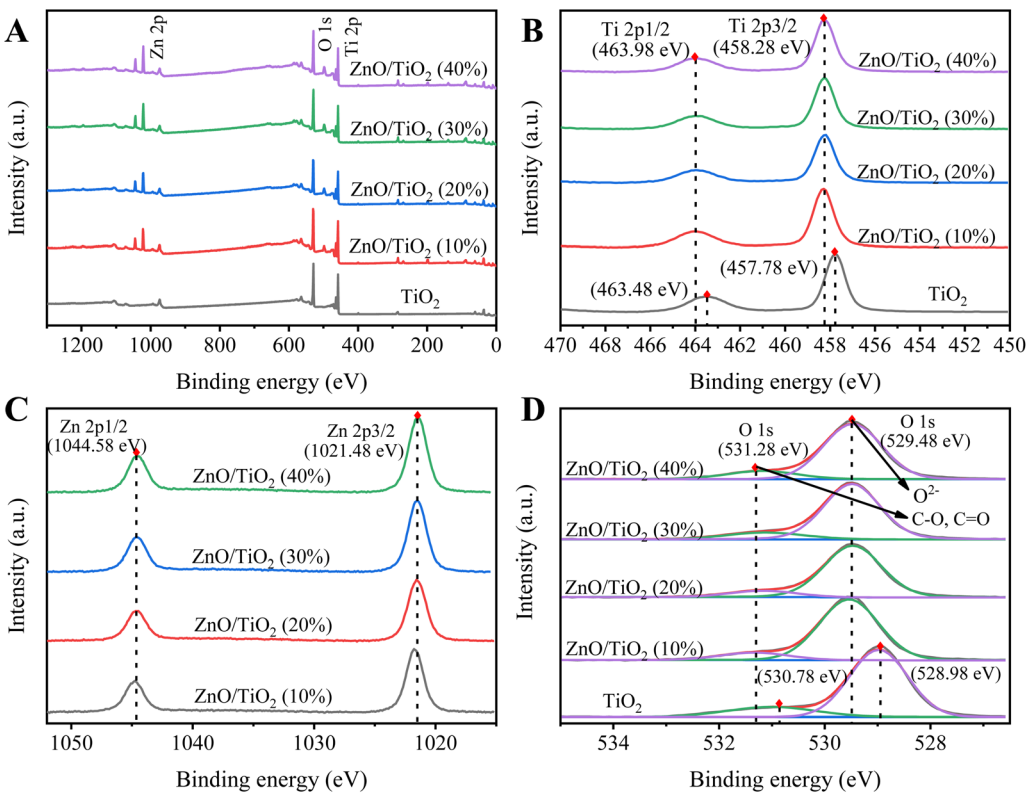

Fig. 2 XPS spectra of ZnO/TiO_2 with different ZnO mass fractions: (a) survey, (b) Ti 2p, (c) Zn 2p, and (d) O 1s.

Table 1 ZnO/TiO_2 ICP, acid content and pore structure with different ZnO mass fractions

	w (Zn)/%						
Catalyst	Measured values of ICP	Measured values of XPS	Theoretical values	Content of acidic site (mmol g^{-1})	S_{BET} (m^2 g^{-1})	Volume (cm^3 g^{-1})	Pore diameter (nm)
TiO_2	—	—	—	0.38	87.23	0.17	10.03
ZnO/TiO_2 (10%)	7.31	10.81	8.03	0.71	54.65	0.13	9.86
ZnO/TiO_2 (20%)	15.10	12.77	16.05	0.51	42.74	0.10	9.46
ZnO/TiO_2 (30%)	22.73	13.65	24.08	0.50	39.26	0.10	8.83
ZnO/TiO_2 (40%)	29.82	14.16	32.10	0.42	36.32	0.09	8.53

Fig. 3. As shown in Fig. 3A, the NH_3-TPD study confirms that catalysts with different ZnO mass fractions have a weak acid site at 100 and 155 °C, and a moderately strong acidic site at 330 °C. Comparing different temperature ranges of desorption peaks, the area of desorption peak in the low temperature rang changes slightly, revealing that loading ZnO has little effect on the strength of the weak acid site; the area of desorption peak in the high temperature rang shows a decreasing trend with the increase of Zn loading, which is possibly due to the fact that part of the strong acid sites on the surface were covered by ZnO and further resulted in decreased strength of strong acid sites. NH_3-TPD results confirm that the strength of strong acid sites on ZnO/TiO_2 samples weakens with the increase of ZnO loading, which is consistent with the results of Giuseppe Marcì *et al.*[31] The band at 1489 cm^{-1} is attributed to a mixture of Lewis and Brønsted acidic sites of pyridine adsorbed;[47] the band at 1539 cm^{-1} is caused by the adsorption of pyridine on the Brønsted acidic site.[48,49] The ratio of Brønsted to Lewis acidic site in ZnO/TiO_2 (20%) catalyst is 0.3, suggesting that ZnO/TiO_2 (20%) is a Lewis acid-based catalyst.

As can be seen from Fig. 4A–E, when the mass fraction of ZnO is 10%, there are clear active component particles on the surface of the catalyst. With the increase of ZnO mass fraction, the agglomeration of particles of the surface-active components of the catalyst was obvious, and the ZnO/TiO_2 (40%) catalyst was the most serious.

It can be seen from Fig. 5 and Table 1 that with the increase of ZnO mass fraction, the specific surface area, pore volume and pore size of the catalyst are reduced, and the specific surface area decreases significantly, which is due to the continuous deposition of ZnO particles on the surface of the support, consistent with the results of SEM and NH_3-TPD. From the N_2 adsorption/desorption curves, it can be seen that the catalyst has a mesoporous structure, which can help the diffusion of raw materials and products on the surface of the catalyst, and change from single-layer adsorption to multi-layer adsorption with the rise of pressure.

3.3 Catalytic performance of ZnO/TiO_2 on transesterification reaction

The catalytic activities of ZnO/TiO_2 catalysts with different ZnO contents can be found in Fig. 6.

When using pure TiO_2 as the catalyst, only a small amount of PCDL was detected and the M_n was only 1404 g mol^{-1}. When the loading amount of ZnO is 10%, the yield and M_n are significantly improved. However, the content of by-product tetrahydrofuran was as high as 8.7% over 10% ZnO/TiO_2. The results should be related to its largest amount of the surface acidic site, because acidic site can also promote the dehydration of BDO to form tetrahydrofuran.[50] To our delight, ZnO/TiO_2 (20%) catalyst with appropriate amount of acidic site gave the highest M_n value of PCDL and good yield. Further increasing the ZnO loading

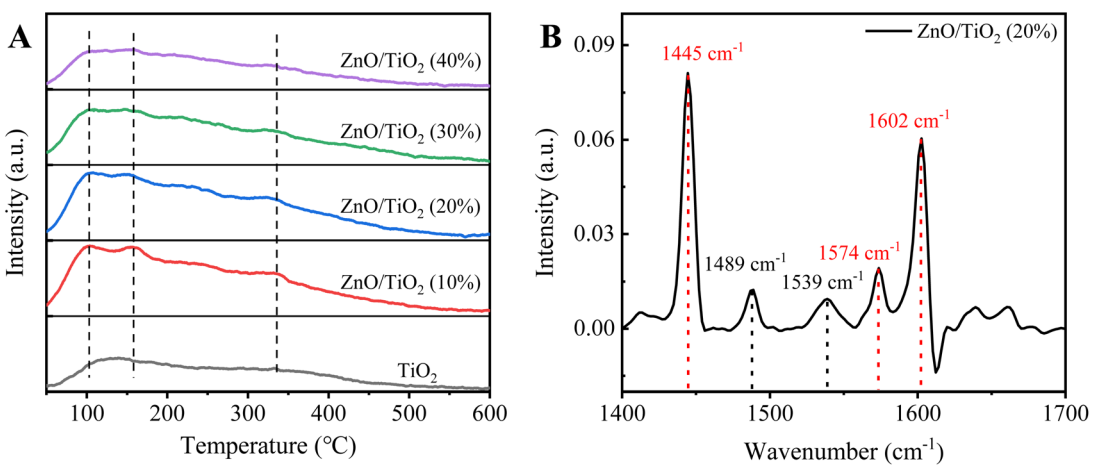

Fig. 3 (A) ZnO/TiO_2 NH_3-TPD with different ZnO mass fractions (B) Py-IR of ZnO/TiO_2 (20%).

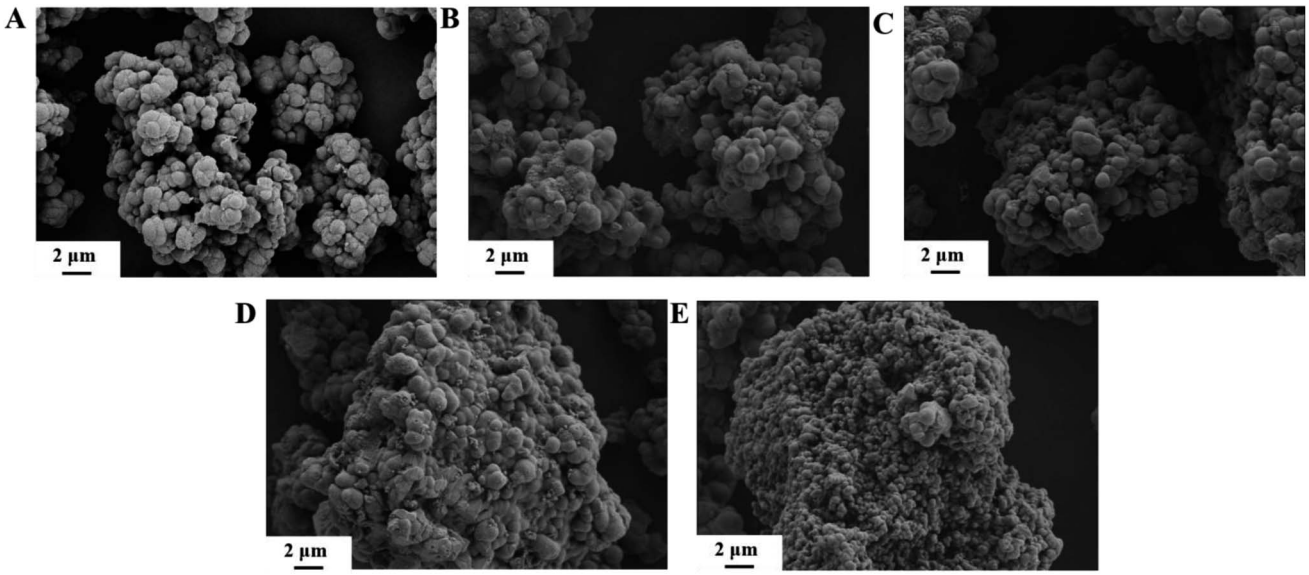

Fig. 4 SEM of (A) 10%, (B) 20%, (C) 30%, (D) 40%, (E) 50% ZnO/TiO_2.

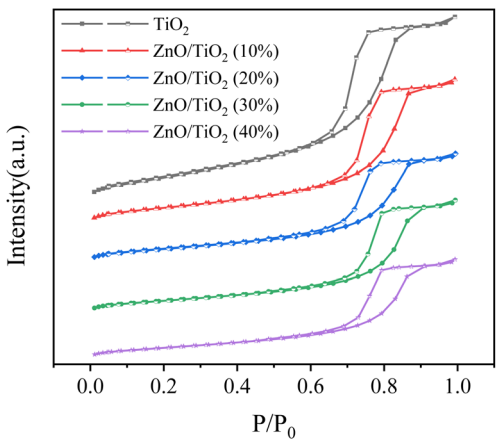

Fig. 5 N_2 adsorption/desorption curves of ZnO/TiO_2 with different ZnO mass fractions.

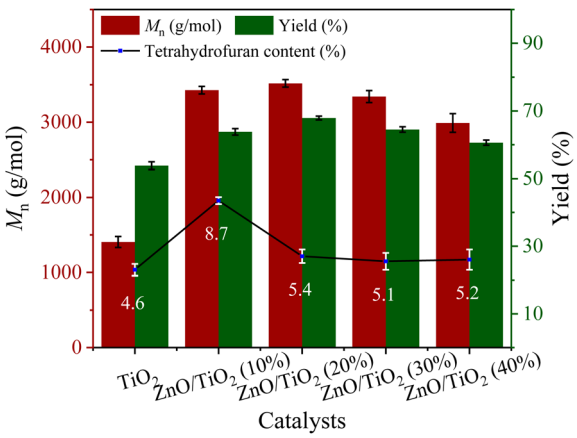

Fig. 6 Effect of ZnO loading on catalyst performance (reaction conditions: DPC : BDO = 1 : 1.1; catalyst amount: 0.3 wt%; transesterification temperature: 200 °C). Data points were mean of triplicate experiments with the error bars showing standard deviations.

amount results in the gradually decease of yield and M_n. It can be seen from the SEM (Fig. 4) that ZnO agglomerates on the surface of TiO_2 for ZnO/TiO_2 (30%) catalyst, and part of the active center of TiO_2 is covered by ZnO, and the synergy between Ti–O–Zn is weakened, so the yield and M_n decreases. Concerning on the PDI, the value changes slightly for all the catalysts except ZnO/TiO_2 (10%). Titanium and zinc oxides are presumed to be active centers of Lewis acid. The carbonyl oxygen in DPC molecule interacts with the Lewis acid active site on ZnO/TiO_2, leading to transfer of electron cloud to ZnO/TiO_2 to form catalyst transition state.[51,52] The reaction enhances the electrophilicity of carbonyl carbon in DPC molecule, and the carbonyl carbon in DPC molecule is more susceptible to the attack of nucleophilic species.[48] Subsequently, C–O is broken, and the intermediate compound S-1 is generated. The intermediate compound S-1 then reacts under the action of Lewis acid active center of ZnO/TiO_2 catalyst to produce PCDL and by-product phenol.[1] The by-product phenol can formed with dimethyl carbonate into the raw material DPC, forming a "zero emission" green process (Scheme 1).[53–55]

3.4 Optimization of process conditions and reusability of catalyst

The ZnO/TiO_2 (20%) catalyst was used to investigate the effect of reaction temperature on the transesterification process. When the transesterification reaction temperature is too low, the reaction rate is slow. And as the vacuum degree continues to increase, the oligomers are pumped away, resulting in low yield and M_n value; when the temperature is too high, the by-product phenol is easier to remove, which further increases the molecular chain of PCDL. However, the high temperature causes thermal degradation of PCDL, and the low molecular weight

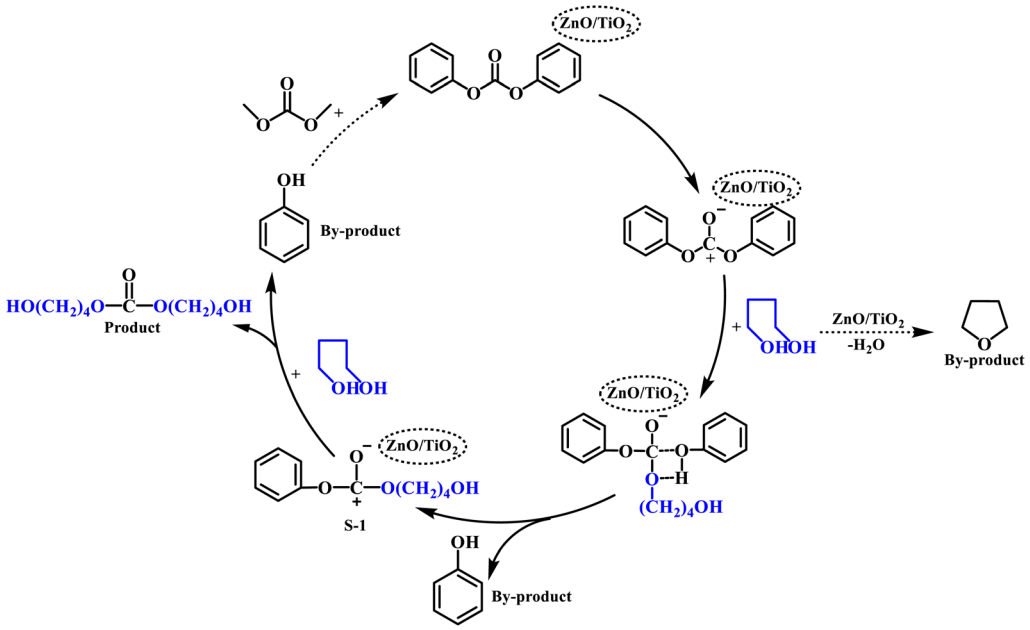

Scheme 1 The possible reaction pathways.

product is pumped away with the increasing vacuum, resulting in a significant decrease in yield. Therefore, the appropriate reaction temperature is 210 °C.

Alcohol excess is conducive to the reaction in a positive direction, the molecular weight distribution becomes smaller. On the other hand, excess alcohol also causes one or both ends

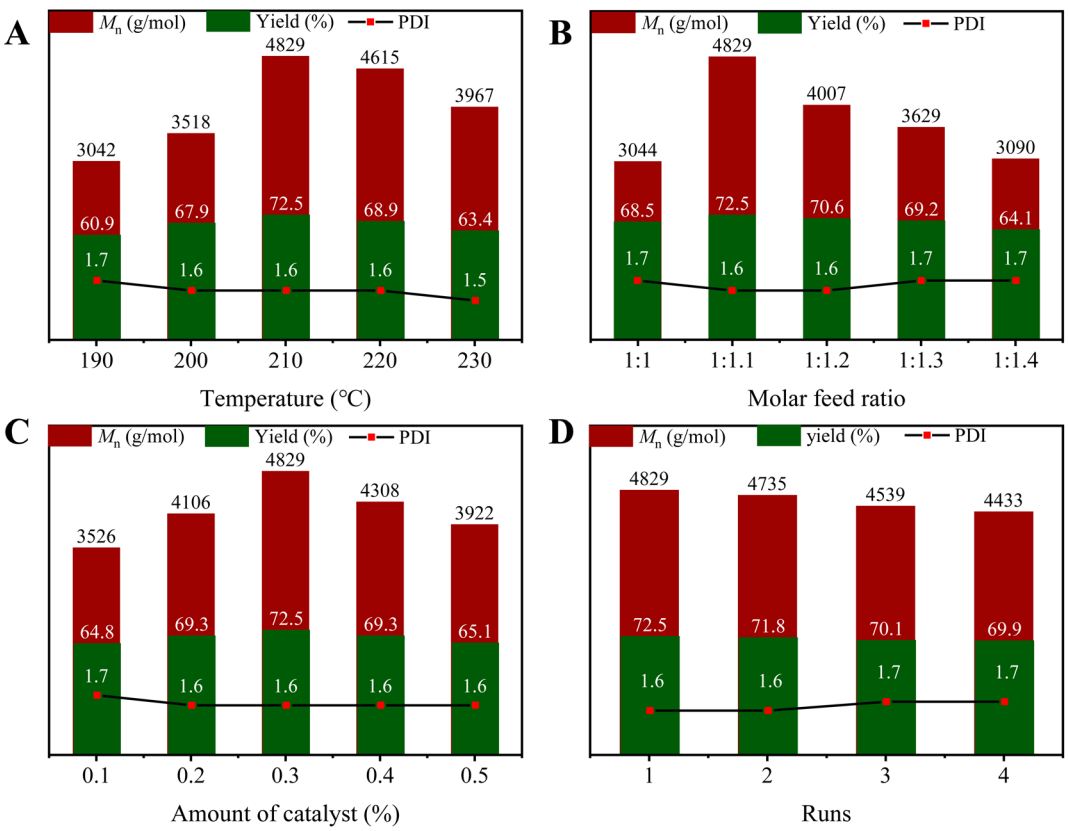

Fig. 7 Effect of (A) transesterification temperature, (B) molar feed ratio and (C) catalyst amount on the M_n, yield and PDI of PCDL; (D) reusability of ZnO/TiO_2 catalysts.

of the product molecular chain to be blocked by ethyl, resulting in lower molecular weight[4] (Fig. 7B). Therefore, the molar feeding ratio of the appropriate raw material is 1 : 1.1.

As depicted in Fig. 7C, the M_n gradually increases with increasing catalyst amount. And the maximum M_n of 4829 g mol^{-1} was reached when the catalyst amount was 0.3%. This is mainly because polycondensation rate is fast at a high catalyst amount. Additionally, the M_n of PCDL decreases from 4829 to 3922 g mol^{-1} with the increase of catalyst amount all the time. On the basis of these results, the most suitable catalyst amount was 0.3%. Song *et al.*[13] reported the synthesis of PCDLs using CH_3COONa as a homogeneous catalyst, with a number average molecular weight of 2800 g mol^{-1} and the yield of PCDL is 64.7% were achieved under the optimum reaction conditions. Feng *et al.*[18] used calcined Mg Al hydrotalcites (HTc) as a solid base catalyst to synthesis PCDL, a high yield of PCDLs up to 95% was obtained, but the molecular weight is only about 1500 g mol^{-1}. The M_n and yield of PCDL prepared by ZnO/TiO_2 (20%) is higher than that of CH_3COONa and Mg Al hydrotalcite. At the same time, the raw materials for the catalyst in this research is readily available, and the reaction process is simple, so the cost of preparing PCDL can be significantly reduced.

The used ZnO/TiO_2 (20%) catalyst was recovered by centrifugation and washed three times with dichloromethane for the next use.[17] It was found that the molecular weight of PCDL decreased slowly with the increase of reuse times. After the catalyst was reused four times, no obvious change of the yield of PCDL was observed. These results indicate that the catalyst has good stability in the synthesis of PCDL.

4. Conclusions

ZnO/TiO_2 catalysts with different ZnO mass fractions were prepared by equal volume impregnation method, characterized and evaluated in the synthesis of polycarbonate diol *via* transesterification. The results showed that with the increase of ZnO mass fraction, the content of surface acidic site decrease, and ZnO/TiO_2 catalyst was dominated by Lewis acidic sites. ZnO/TiO_2 (20%) catalyst appropriate amount of acidic site showed the best catalytic performance. Furtherly, the transesterification process for the synthesis of PCDL was optimized, and the M_n reached 4829 g mol^{-1} with a yield of 72.5% under the optimized conditions. Compared with the reported metal catalysts for the synthesis of polycarbonate diol *via* transesterification, the ZnO/TiO_2 (20%) catalyst is cheaper and easier in preparation.

Author contributions

Ran Chong: investigation, data curation, methodology, writing-original draft. Fei Qian: investigation, data curation. Zhong-Hua Sun: data curation, funding acquisition, writing-review & editing, conceptualization. Mei-Jun Wei: investigation, methodology. Wei-You Zhou: conceptualization, methodology. Ming-Yang He: supervision, validation. Qun Chen: supervision, conceptualization. Jun-Feng Qian: conceptualization, funding acquisition, writing-review & editing.

Conflicts of interest

The authors declare no conflict of interest.

Acknowledgements

We gratefully acknowledge the financial support from A Project Funded by the Priority Academic Program Development of Jiangsu Higher Education Institutions (PAPD) and Jiangsu Key Laboratory of Advanced Catalytic Materials and Technology (Grant BM2012110).

Notes and references

1 L. Wang, J. He, X. Chen and Y. Lv, *J. Iran. Chem. Soc.*, 2020, **17**, 2335–2343.
2 H. Fang, H. Wang, J. Sun, H. Wei and Y. Ding, *RSC Adv.*, 2016, **6**, 13589–13599.
3 K. Fukushima and K. Nozaki, *Macromolecules*, 2020, **53**, 5018–5022.
4 X.-Q. Wang, H. Li, Q.-Y. Yuan, X.-Q. Liu and D.-H. Liu, *Catal. Lett.*, 2020, **150**, 3174–3183.
5 H.-I. Mao, C.-W. Chen, L.-Y. Guo and S.-P. Rwei, *J. Appl. Polym. Sci.*, 2022, **139**, e52986.
6 W. Yu, E. Maynard, V. Chiaradia, M. C. Arno and A. P. Dove, *Chem. Rev.*, 2021, **121**, 10865–10907.
7 J. Sun and D. Kuckling, *Polym. Chem.*, 2016, **7**, 1642–1649.
8 L. Wang, B. Xiao, G. Wang and J. Wu, *Sci. China: Chem.*, 2011, **54**, 1468–1473.
9 Y. Wang, L. Yang, X. Peng and Z. Jin, *RSC Adv.*, 2017, **7**, 35181–35190.
10 M. Honda and H. Abe, *Green Chem.*, 2018, **20**, 4995–5006.
11 S. Tempelaar, L. Mespouille, O. Coulembier, P. Dubois and A. P. Dove, *Chem. Soc. Rev.*, 2013, **42**, 1312–1336.
12 L. Zhu, W. Xue and Z. Zeng, *New J. Chem.*, 2018, **42**, 15997–16004.
13 M. Song, X. Yang and G. Wang, *Chem. Res. Chin. Univ.*, 2018, **34**, 578–583.
14 Z. Terzopoulou, E. Karakatsianopoulou, N. Kasmi, V. Tsanaktsis, N. Nikolaidis, M. Kostoglou, G. Z. Papageorgiou, D. A. Lambropoulou and D. N. Bikiaris, *Polym. Chem.*, 2017, **8**, 6895–6908.
15 Z. Wang, X. Yang, S. Liu, J. Hu, H. Zhang and G. Wang, *RSC Adv.*, 2015, **5**, 87311–87319.
16 Z. Wang, X. Yang, S. Liu, H. Zhang and G. Wang, *Chem. Res. Chin. Univ.*, 2016, **32**, 512–518.
17 M. Song, X. Yang and G. Wang, *RSC Adv.*, 2018, **8**, 35014–35022.
18 Y. X. Feng, N. Yin, Q. F. Li, J. W. Wang, M. Q. Kang and X. K. Wang, *Ind. Eng. Chem. Res.*, 2008, **47**, 2140–2145.
19 Z. Wang, X. Yang, J. Li, S. Liu and G. Wang, *J. Mol. Catal. A: Chem.*, 2016, **424**, 77–84.
20 Y.-K. Yang, S.-W. Yoon, Y.-T. Hwang and B.-G. Song, *Bull. Korean Chem. Soc.*, 2012, **33**, 3445–3447.
21 K. Stępień, C. Miles, A. McClain, E. Wiśniewska, P. Sobolewski, J. Kohn, J. Puskas, H. D. Wagner and M. El Fray, *ACS Sustainable Chem. Eng.*, 2019, **7**, 10623–10632.

22 Y. Liang, K. Su, L. Cao and Z. Li, *Mol. Catal.*, 2019, **465**, 16–23.
23 X. Chen, Y. Huang, Y. Li, H. Li, G. Fan, R. Zhang and X. Xu, *Mater. Lett.*, 2021, **293**, 129709–129713.
24 S. Yurdakal, Ş. Ö. Yanar, S. Çetinkaya, O. Alagöz, P. Yalçın and L. Özcan, *Appl. Catal., B*, 2017, **202**, 500–508.
25 T. Zhang, S. Wang and F. Chen, *J. Phys. Chem. C*, 2016, **120**, 9732–9739.
26 S. Ahadi, N. S. Moalej and S. Sheibani, *Solid State Sci.*, 2019, **96**, 105975–105985.
27 B. Bozkurt Çırak, B. Caglar, T. Kılınç, S. Morkoç Karadeniz, Y. Erdoğan, S. Kılıç, E. Kahveci, A. Ercan Ekinci and Ç. Çırak, *Mater. Res. Bull.*, 2019, **109**, 160–167.
28 T. A. Dontsova, O. I. Yanushevska, S. V. Nahirniak, A. S. Kutuzova, G. V. Krymets, P. S. Smertenko and S. Ali, *J. Chem.*, 2021, **2021**, 1–11.
29 J. Hou, Y. Wang, J. Zhou, Y. Lu, Y. Liu and X. Lv, *Surf. Interfaces*, 2021, **22**, 100889–100896.
30 R. Madhuvilakku and S. Piraman, *Bioresour. Technol.*, 2013, **150**, 55–59.
31 G. Marcì, V. Augugliaro, M. J. López-Muñoz, C. Martín, L. Palmisano, V. Rives, M. Schiavello, R. J. D. Tilley and A. M. Venezia, *J. Phys. Chem. B*, 2001, **105**, 1033–1040.
32 M. Pérez-González and S. A. Tomás, *Catal. Today*, 2021, **360**, 129–137.
33 D. Tekin, H. Kiziltas and H. Ungan, *J. Mol. Liq.*, 2020, **306**, 112905–112911.
34 C. Chen, L. Cai, X. Shangguan, L. Li, Y. Hong and G. Wu, *R. Soc. Open Sci.*, 2018, **5**, 181331.
35 M. M. A. Soliman, A. Karmakar, E. C. B. A. Alegria, A. P. C. Ribeir, G. M. D. M. Rúbio, M. S. Saraiva, M. F. C. G. d. Silva and A. J. L. Pombeiro, *Catal. Today*, 2020, **348**, 72–79.
36 L. Yang, Z. Yang, F. Zhang, L. Xie, Z. Luo and Q. Zheng, *Polymers*, 2018, **10**, 796–815.
37 S. Yu and H. Zhang, *Catal. Lett.*, 2020, **150**, 3359–3367.
38 J. Yang, C. Hu, Y. Jin, H. Chen, W. Zhu and X. Zhou, *Res. Chem. Intermed.*, 2021, **47**, 3453–3468.
39 S. Ponnada, D. B. Gorle, M. S. Kiai, S. Rajagopal, R. K. Sharma and A. Nowduri, *Adv. Mater.*, 2021, **2**, 5986–5996.
40 X. Zhao, C. Peng and J. You, *J. Therm. Spray Technol.*, 2017, **26**, 1301–1307.
41 A. Kutuzova, T. Dontsova and W. Kwapinski, *J. Inorg. Organomet. Polym. Mater.*, 2020, **30**, 3060–3072.
42 Y. Yu, J. Wang, W. Li, W. Zheng and Y. Cao, *CrystEngComm*, 2015, **17**, 5074–5080.
43 M. Zhu, X. Deng, X. Lin, L. Zhang, W. Zhang, Y. Lv and J. Pan, *J. Mater.*, 2018, **29**, 11449–11456.
44 H.-T. Wang, Y.-P. Liu, H. Zhang, N. Chang, W. Shao, M.-S. Shi, D. Ao and M.-C. Lu, *Microporous Mesoporous Mater.*, 2019, **288**, 109548–109557.
45 Y. Wang, X. Liu, L. Guo, L. Shang, S. Ge, G. Song, N. Naik, Q. Shao, J. Lin and Z. Guo, *J. Colloid Interface Sci.*, 2021, **599**, 566–576.
46 F. Xiao, *J. Mater. Chem.*, 2012, **22**, 7819–7830.
47 M. A. A. Aziz, K. Puad, S. Triwahyono, A. A. Jalil, M. S. Khayoon, A. E. Atabani, Z. Ramli, Z. A. Majid, D. Prasetyoko and D. Hartanto, *Chem. Eng. J.*, 2017, **316**, 882–892.
48 Y. Mao, J. Cheng, H. Guo, Y. Shao, L. Qian and W. Yang, *Fuel*, 2023, **331**, 125795–125808.
49 W. Xiang, C. Shen, Z. Lu, S. Chen, X. Li, R. Zou, Y. Zhang and C.-j. Liu, *Chem. Eng. Sci.*, 2021, **233**, 116429–116440.
50 H. Li, H. Yin, T. Jiang, T. Hu, J. Wu and Y. Wada, *Catal. Commun.*, 2006, **7**, 778–782.
51 W. Shi, J. Zhao, X. Yuan, S. Wang, X. Wang and M. Huo, *Chem. Eng. Technol.*, 2012, **35**, 347–352.
52 H. Yang, Z. Xiao, Y. Qu, T. Chen, Y. Chen and G. Wang, *Res. Chem. Intermed.*, 2017, **44**, 799–812.
53 Z. Xiao, H. Yang, H. Zhang, T. Chen and G. Wang, *Chem. Pap.*, 2018, **72**, 2347–2352.
54 J. Zhang, Y. Gao, J. Zhang, J. Zhao and H. Shen, *Chem. Cent. J.*, 2018, **12**, 104–112.
55 Y. Zhang, S. Wang, Z. Xiao, T. Chen and G. Wang, *Res. Chem. Intermed.*, 2016, **42**, 7213–7222.